

# Area-Based Tests of Long-Term Seismic Hazard Predictions

by Steven N. Ward

**Abstract** This article develops several area-based tests of long-term seismic hazard predictions. The tests stem from the hypothesis that the observed fractional area of hazard exceedence should follow in proportion to the region's predicted likelihood of exceedence. For example, a prediction is successful if roughly 30% of the area mapped as having a 30% likelihood of exceeding some hazard threshold in a certain time interval, actually does suffer this level of shaking. Although tests of earthquake predictions are always equivocal, the success or failure of a forecast hazard map can be argued strongly from a statistical assessment of the hundreds of individual point predictions comprising the map. The specific forecasts to be examined are the 30-yr probabilities of peak ground acceleration exceedence that were presented by Ward (1994) for southern California. In lieu of a lengthy historical set of recorded peak accelerations, observational data for the tests were derived from the 150-yr earthquake catalog and standard attenuation relationships. In all cases, the observed hazard ratios were highly correlated with the predictions. Within 95% confidence bounds, the observed levels of hazard coincided with the predicted hazard from models that included a low-magnitude cutoff of  $M = 5.5$  to 6, approximately the same limit as enlisted in the earthquake catalog. I propose a pass/fail criterion for acceleration hazard maps and I suggest that all seismic hazard predictions submit to area-based tests.

## Introduction

Recently, I presented a set of long-term earthquake hazard maps for southern California derived from multi-disciplinary information spanning geology, space geodesy, paleoseismology, observed seismicity, and synthetic seismicity (Ward, 1994). Figures 1a and 1b sample these predictions. The hazard maps contour  $P_{30}^{\text{pred}}(x, a)$ , the 30-yr probability of exceeding peak ground accelerations of  $a = 0.1 g$  and  $0.2 g$  on rock sites from earthquakes of magnitude greater than 5.5 (Fig. 1a) and 6 (Fig. 1b). Undeniably, in constructing the maps, many assumptions were required to merge information from diverse origins and sample time scales. Although the assumptions involved in the melding were as self-consistent as possible, peer reviewers formulated a challenge to the maps that motivates this article.

"Given any existing or hypothetical data set, how do you propose to test these hazard predictions?"

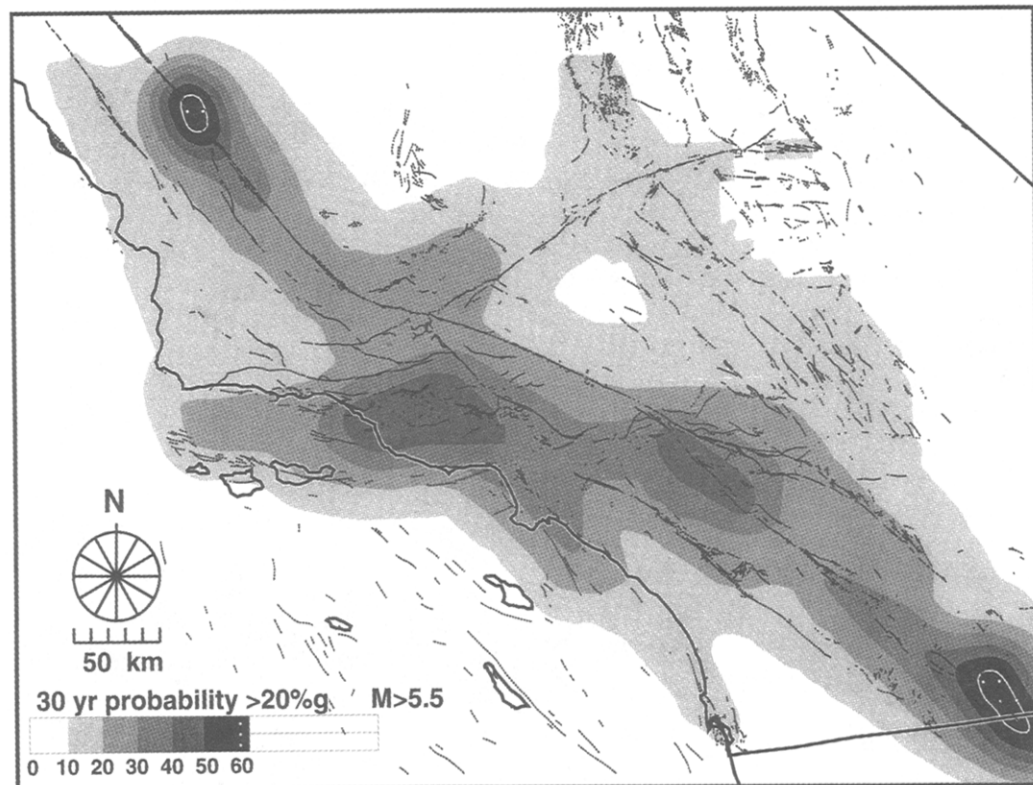
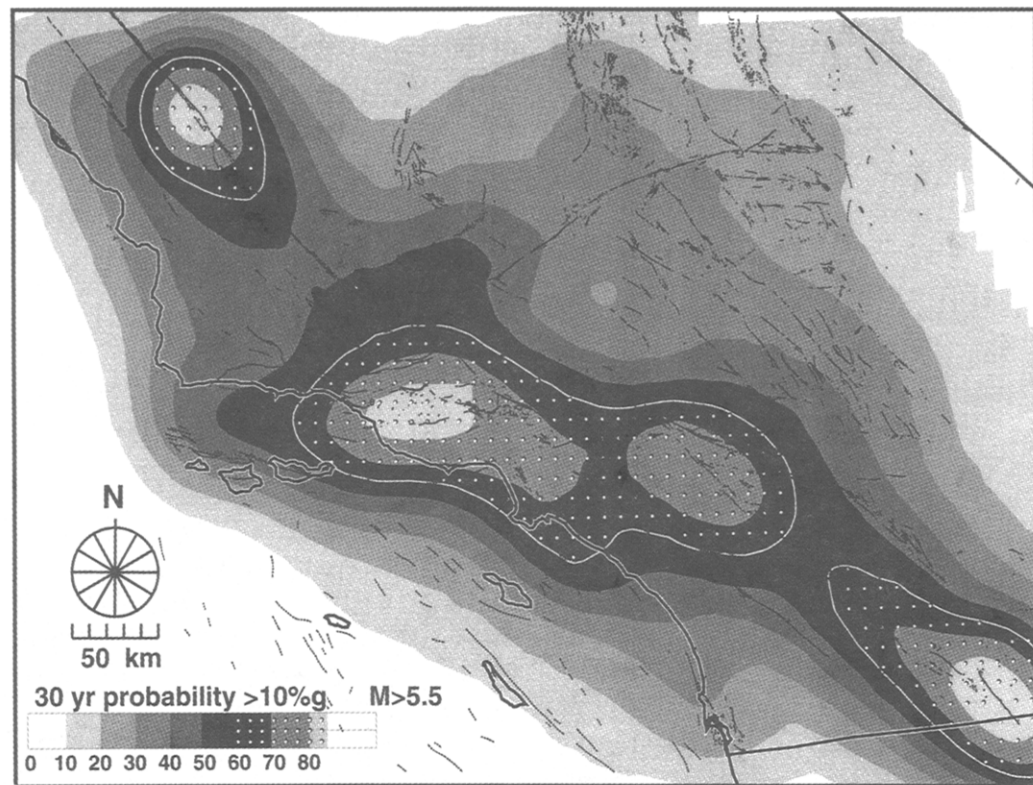
Historically, scientists have offered isolated earthquake predictions in the form "Event  $W$  has an  $X\%$  probability of occurring at location  $Y$  within  $Z$  years." Examples include the Parkfield prediction (Bakun and Lindh, 1985) and the predictions of San Andreas Fault earthquakes by the Working Group on California Earthquake Predictions (WGCEP, 1988, 1990). Unfortunately, the charge of testing isolated predictions has been a bane to seismology. The difficulty is obvious; at best, event  $W$  does happen or it does not. (Let's

not even talk about equivocal situations where an event "almost like"  $W$  occurred "close to"  $Y$ .) In either case, the prediction is neither proved nor disproved for any but the most extreme values of  $W$ ,  $X$ ,  $Y$ , or  $Z$ .

Given the vulgarities of testing even a single  $X$ ,  $Y$ ,  $Z$  prediction (and putting the data question aside for the moment), how can the above challenge be met for hazard forecasts involving the whole of southern California? Surprisingly perhaps, compared to an isolated earthquake prediction, the areal nature of the hazard forecast can be played to advantage. True, at any given point (say, one inside the black area in the top of Fig. 1a), the forecast takes a  $X$ ,  $Y$ ,  $Z$  form—"Accelerations exceeding  $0.1 g$  have a 50 to 60% probability of occurring here within 30 yr." The distinction however, is that the hazard maps make corresponding predictions at hundreds of points. Multiplicity provides a leg up in that the occurrence or nonoccurrence of event  $W$  can now be viewed in the spectrum of all similar predictions. Unlike an isolated earthquake prediction where statistical uncertainty clouds conclusions, statistics here can be an ally.

This article proposes some area-based tests of seismic hazard maps and, in lieu of a lengthy historical record of observed accelerations, constructs and uses data sets derived from the earthquake catalog.

(a)



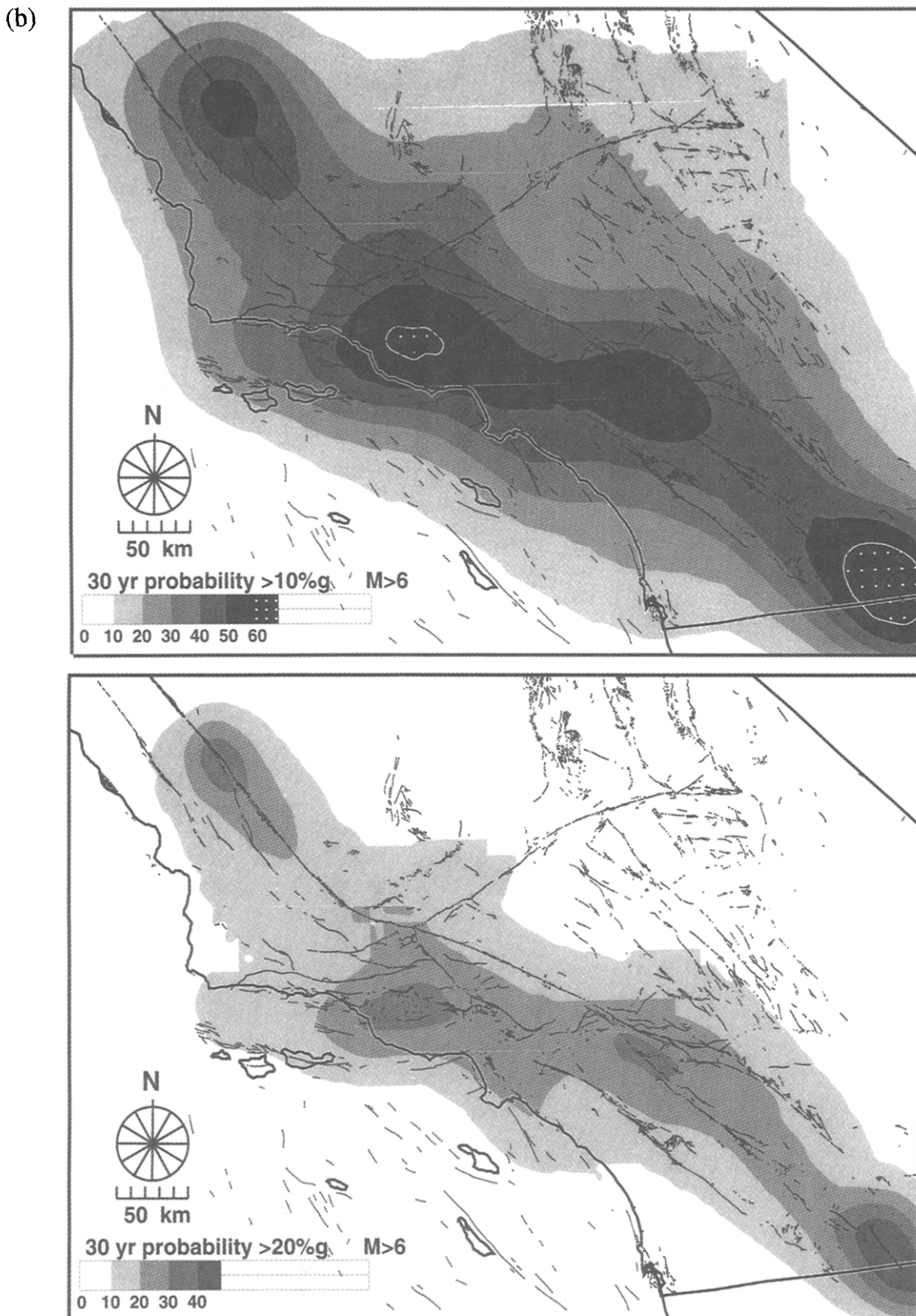


Figure 1. (a) Map of southern California showing predicted 30-yr probabilities  $P_{30}^{\text{pred}}(x, a)$  of exceeding accelerations of  $a = 0.1 \text{ g}$  (top) and  $0.2 \text{ g}$  (bottom) from earthquakes  $M \geq 5.5$ .  $P_{30}^{\text{pred}}(x, a)$  drops as the specified exceedence level  $a$ , or low-magnitude cutoff increases. (b) Map of southern California showing predicted 30-yr probabilities  $P_{30}^{\text{pred}}(x, a)$  of exceeding accelerations of  $a = 0.1 \text{ g}$  (top) and  $0.2 \text{ g}$  (bottom) from earthquakes  $M \geq 6$ .

## The Acceleration Data Base

Because the hazard maps take the form of 30-yr probabilities of exceedence of some level of acceleration, the most appropriate data to test the predictions would be observed peak accelerations (suitably corrected to bedrock) for sites covering southern California for the last 30 yr, the next 30 yr, or better yet, several 30-yr intervals. Seeing, however, that existing data are too sparse geographically to be of much use, and conceding that at my age it is impractical to wait for 30 more years of measurements to accumulate, the tests will have to be performed on acceleration data that have been generated from earthquake catalogs. Critics might claim that generating “observations” is cheating. Granted, synthetic acceleration data inferred from existing seismicity catalogs cannot be an authoritative test of ground-motion levels predicted for future earthquakes because the synthetic data and the hazard maps share the same, possibly inadequate, attenuation relation, and because the mere consistency of past events with the predictions is no guarantee of their reliability. Still, I argue that this course falls within the purview of the challenge, and that if they wish, younger seismologists can implement the tests with “real” acceleration data when it becomes available.

The parent earthquake catalog that was used to generate the acceleration data was published by Ellsworth (1990) and spans the years 1850 to 1987. A few larger events that occurred after 1988 were added, as well as a handful of southern California quakes listed in Yerkes (1985) but not included by Ellsworth. Although the catalog contains a smattering of earthquakes down to  $M = 5.2$ , it is viewed to be complete for the San Andreas Fault system to  $M = 6$ . For southern California, the completeness of the catalog may stretch a few tenths of a magnitude unit lower.

Using the Joyner and Boore (1981) attenuation equations for peak ground acceleration  $A_p(M, D)$  on rock sites, and the catalog epicentral distances  $D$  and earthquake magnitudes  $M$ , I generated “observed” 150-yr exceedence area maps for accelerations of  $a = 0.1 \text{ g}$  and  $0.2 \text{ g}$  (Fig. 2). The speckles in this figure cover regions where  $A_p(M, D) > a$  for at least one of the catalog earthquakes (*large stars*). I note that in formulating the observed acceleration data base, finite faults (with the exceptions of the 1857 and the 1872 ruptures) were idealized as point sources. To some extent, however, the effect of fault length has been taken into account by using a modified source distance  $D(M)$ , that depends on magnitude (see Ward, 1994, Appendix B for details). This same attenuation relation and distance correction was used to construct the hazard maps.

### 150-Yr Exceedence Area-Probability Test

The predicted probability contours,  $P_{30}^{\text{pred}}(\mathbf{x}, a)$ , in the hazard maps of Figure 1 vary smoothly because they include the scaled effects of earthquakes with repeat times of hundreds or even thousands of years. In any 30- or 150-yr pe-

riod, earthquake occurrence is poorly sampled, so comparable observed probabilities  $P_T^{\text{obs}}(\mathbf{x}, a)$  will be rougher geographically, with peaks centered at locations that happened to have experienced a quake in that time interval. Nevertheless, if the hazard maps have any validity, it is reasonable to suppose that the observed likelihood of exceeding a threshold acceleration *averaged over an area A* should follow in proportion to the predicted likelihood, in particular

$$P_T^{\text{pred}}(A, a) \approx P_T^{\text{obs}}(A, a), \quad (1)$$

with

$$P_T^{\text{pred}}(A, a) = (1/A) \int_{A(\mathbf{x})} P_T^{\text{pred}}(\mathbf{x}, a) dA(\mathbf{x}) \quad (2a)$$

$$P_T^{\text{obs}}(A, a) = (1/A) \int_{A(\mathbf{x})} P_T^{\text{obs}}(\mathbf{x}, a) dA(\mathbf{x}). \quad (2b)$$

The areas  $A$  covered in the integrals are arbitrary, but they should be large enough to insure stable estimates of  $P_T^{\text{pred}}(A, a)$  and  $P_T^{\text{obs}}(A, a)$  if the difficulties associated with verifying an isolated prediction are to be minimized.

When the observational data are exceedence area maps like Figure 2, then  $P_T^{\text{obs}}(\mathbf{x}, a)$  is either 0 or 1, and equation (1) reduces to a simple area test. Area tests are easy to understand. For instance, the blackened region in the top of Figure 1a includes points with 50 to 60% likelihood of experiencing accelerations exceeding  $0.1 \text{ g}$  in 30 yr. For any 30 yr of observations then, 50 to 60% of the blackened area should actually record accelerations of  $0.1 \text{ g}$  or more. The same is true for the other contours—accelerations exceeding  $0.1 \text{ g}$  should occur in 20 to 30% of the area between the 20 and 30% probability contours; in 80 to 90% of the area between the 80 and 90% contours; etc.

To set the stage for the area test, the different time intervals for Figure 1 (30 yr) and Figure 2 (150 yr) must be reconciled. Either the predictions have to be scaled to a longer interval or the observations have to be scaled to a shorter one. Being Poissonian, the hazard maps are not specific to any 30-yr period, so it is easy to obtain 150-yr predicted probabilities  $P_{150}^{\text{pred}}(\mathbf{x}, a)$  from the 30-yr values  $P_{30}^{\text{pred}}(\mathbf{x}, a)$  by

$$P_{150}^{\text{pred}}(\mathbf{x}, a) = 1 - [1 - P_{30}^{\text{pred}}(\mathbf{x}, a)]^{150/30}. \quad (3)$$

Figures 3a and 3b map  $P_{150}^{\text{pred}}(\mathbf{x}, 0.1 \text{ g})$  and  $P_{150}^{\text{pred}}(\mathbf{x}, 0.2 \text{ g})$  with low-magnitude cutoffs of 5.5 and 6. The 150-yr likelihoods are, of course, much greater than the 30-yr values in Figure 1.

Figure 4 plots area-averaged probabilities  $P_{150}^{\text{obs}}(A_j, a)$  versus  $P_{150}^{\text{pred}}(A_j, a)$  for the 10 areas  $A_j$  between adjacent predicted contours (0 to 10%, 10 to 20%, 20 to 30%, etc.) of Figure 3. The left and right columns of the figure use thresholds of  $a = 0.1 \text{ g}$  and  $a = 0.2 \text{ g}$ , and the three rows compare hazard maps with low-magnitude cutoffs of  $M \geq 5$  (Fig. 10,

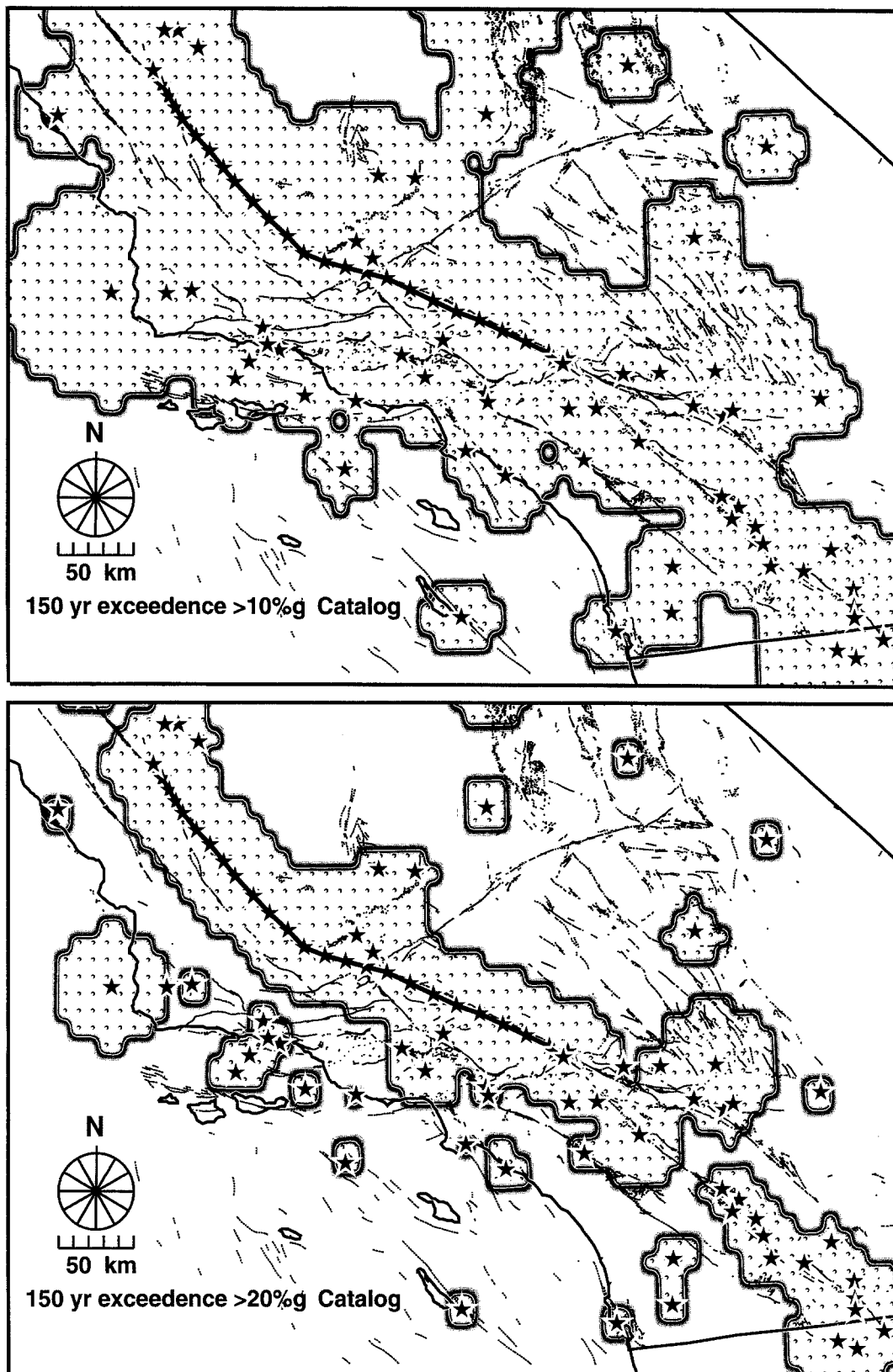
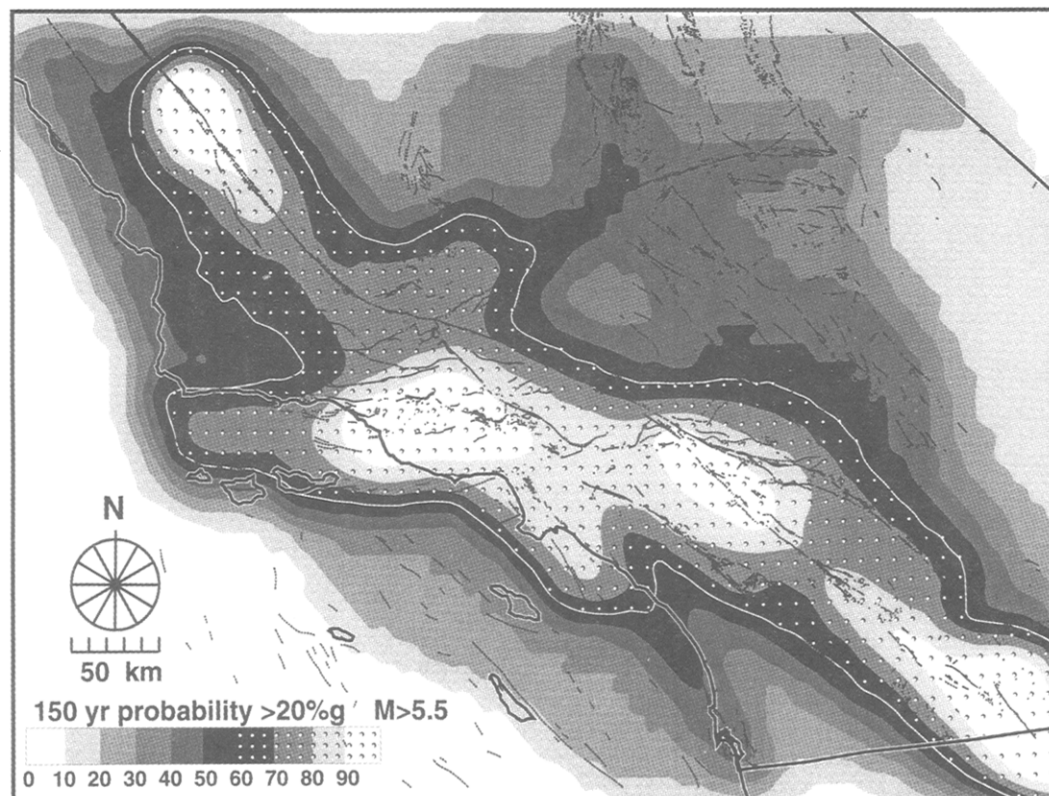
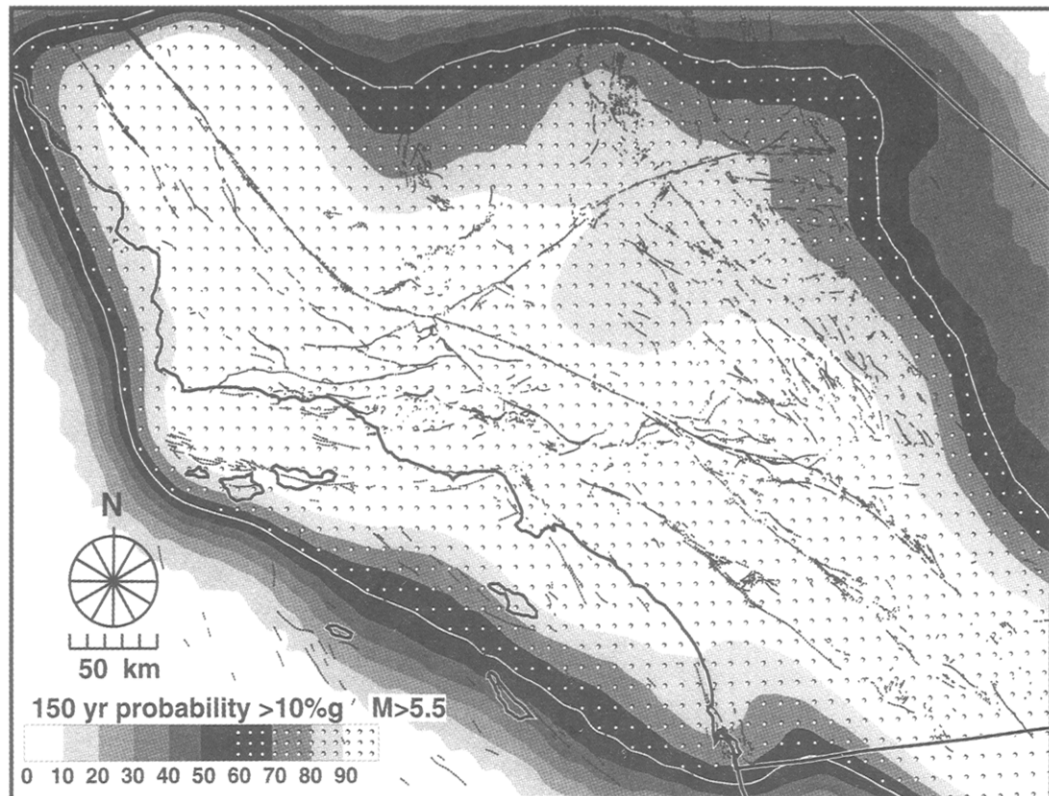
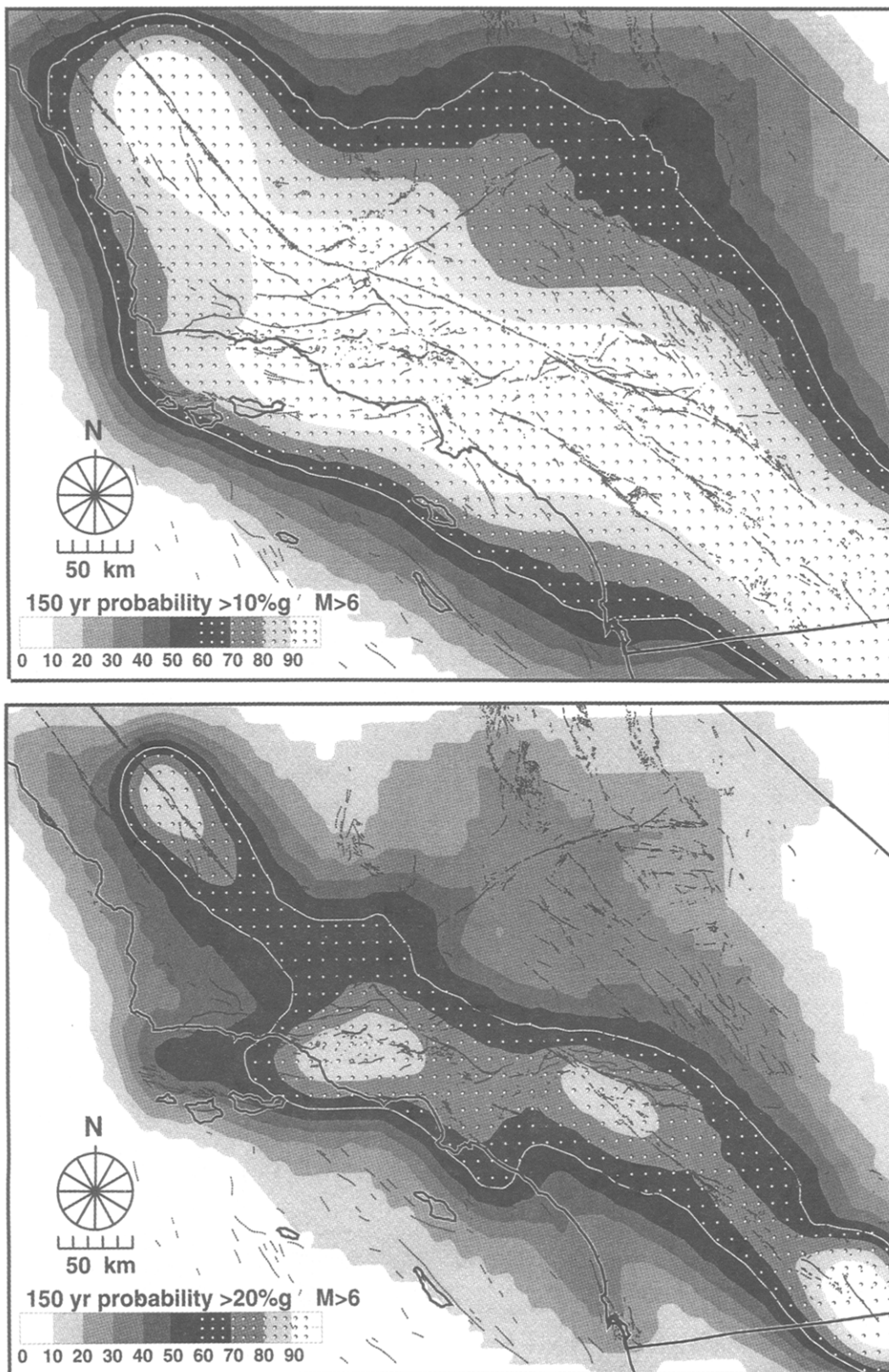


Figure 2. Observed 150-yr exceedence area maps for accelerations of  $0.1\text{ g}$  (top) and  $0.2\text{ g}$  (bottom) based on the earthquake catalog and the Joyner and Boore (1981) attenuation curves. Speckled areas should have suffered accelerations exceeding the threshold values from at least one of the catalog events (stars).

(a)



(b)



**Figure 3.** (a) Predicted 150-yr probabilities  $P_{150}^{\text{pred}}(\mathbf{x}, a)$  of exceeding accelerations of  $a = 0.1 \text{ g}$  (top) and  $0.2 \text{ g}$  (bottom) from earthquakes  $M \geq 5.5$ . These probabilities were scaled from  $P_{50}^{\text{pred}}(\mathbf{x}, a)$  using equation (3). (b) Predicted 150-yr probabilities  $P_{150}^{\text{pred}}(\mathbf{x}, a)$  of exceeding accelerations of  $a = 0.1 \text{ g}$  (top) and  $0.2 \text{ g}$  (bottom) from earthquakes  $M \geq 6$ . These probabilities were scaled from  $P_{50}^{\text{pred}}(\mathbf{x}, a)$  using equation (3).

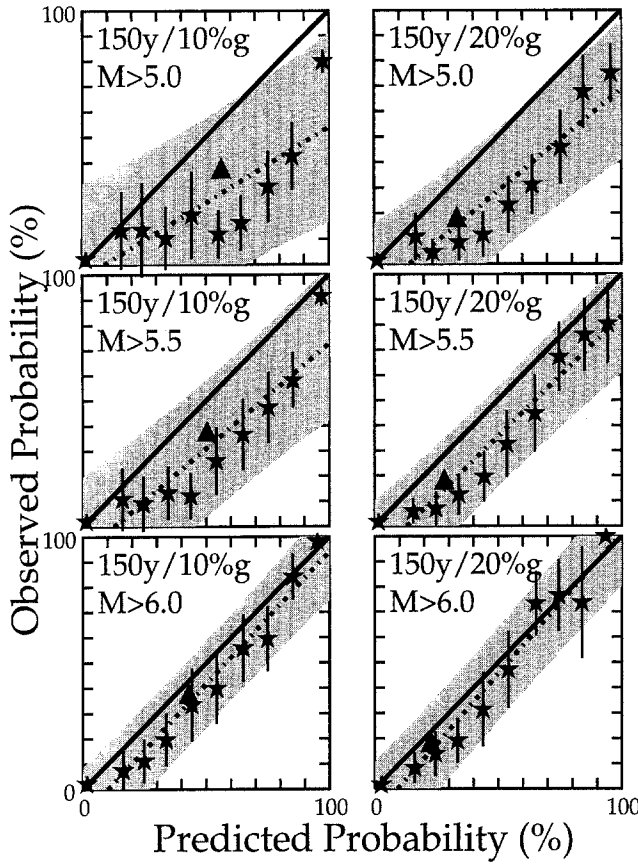


Figure 4. Observed versus predicted 150-yr area-averaged probabilities (Fig. 3 versus Fig. 2). The 10 averaging areas lie between adjacent 10% contours of  $P_{150}^{\text{pred}}(\mathbf{x}, a)$ . Left and right columns compare accelerations of 0.1 g and 0.2 g. From top to bottom, the rows test predictions with low-magnitude cutoffs of  $M \geq 5$ , 5.5, and 6. Note the strong correlation between observations and predictions. The shaded area is the 95% confidence region surrounding the best linear fit to the data (dashed line). Poorer fit to the predicted hazard levels (diagonal solid line) with decreasing magnitude cutoff is a consequence of the incompleteness of the observed catalog. The large triangles plot  $P_{150}^{\text{obs}}(A_{\text{total}}, a)$  versus  $P_{150}^{\text{pred}}(A_{\text{total}}, a)$  for all of southern California.

Ward, 1994),  $M \geq 5.5$  (Fig. 1a), and  $M \geq 6$  (Fig. 1b). The vertical lines through the stars span the estimated 95% confidence interval on  $P_{150}^{\text{obs}}(A_j, a)$  based on the number of grid points  $n_j$  in each  $A_j$ , as  $\pm 1.96 \sqrt{P_{150}(1 - P_{150})/n_j}$ . The  $n_j$  represents the number of independent estimates of  $P_{150}^{\text{obs}}(\mathbf{x}, a)$  in each area  $A_j$ . Because the  $P_{150}^{\text{obs}}(\mathbf{x}, a)$  are correlated across some distance  $l_c$ ,  $n_j$  must be less than  $n_j$  roughly like  $n_j' = A_j/(\delta A + l_c^2)$ , where  $\delta A$  is the area of the grid elements. Decreasing  $\delta A$  much below the squared correlation length no longer helps to reduce the error in the estimate of the mean value,  $P_{150}^{\text{obs}}(A_j, a)$ . I took  $l_c$  to be 20 km, about twice the typical faulting depth of earthquakes. The shaded confidence region surrounding the best regression line (dashed) is proposed to cover 95% of the existing and future data points

(see Montgomery and Rung, 1994, pp. 501–503). Without doubt, a strong positive correlation exists between the observations and predictions. Correlation coefficients for the best linear fit to the data range between 0.80 and 0.98. The likelihood that the randomly drawn hazard contours would contribute to such a correlation is far less than 1%.

Where the stars fall below the diagonal line in Figure 4, the predicted shaking hazard exceeds the observed level. Predictions employing a low-magnitude cutoff of  $M \geq 6$  best fit the data. As the magnitude cutoff decreases, the model overpredicts the hazard computed from the catalog. This trend could be expected in view of the fact that the source of the data is complete only to  $M = 6$ . Although they are probably closer to reflecting true hazard, predictions that include progressively smaller earthquakes should progressively overstate the hazard inferred from the Ellsworth catalog.

### 150-Yr Probability–Probability Test

If nothing else, the area test confirms that regions of high predicted hazard are strongly correlated with regions of high observed hazard. Of course, “high” and “low” are relative terms and it is necessary to extend the test to determine whether observed and predicted hazards possess the same numerical scale. Figure 4 indicates that while there is a strong correlation between  $P_{150}^{\text{obs}}(A_j, a)$  and  $P_{150}^{\text{pred}}(A_j, a)$ , there is a bias toward overprediction even with an  $M = 6$  cutoff. Partly the bias occurs because the area-probability test is not quite comparing oranges to oranges. In the hazard maps, account was taken for the uncertainty in the attenuation law; that is, the finite likelihood that an earthquake of a certain distance and magnitude will produce an acceleration larger or smaller than the average value,  $A_p(M, D)$ . The hazard maps allowed for a Gaussian spread of 0.22 in  $\log [A_p(M, D)]$ . Effectively, this affords the smaller, but more numerous, quakes a greater role in shaking probabilities than they would have otherwise. An improved test employs observed accelerations computed from the catalog, but includes the uncertainty in the attenuation law. The new probabilities  $P_{150}^{\text{obs}}(\mathbf{x}, a)$  are determined by

$$P_{150}^{\text{obs}}(\mathbf{x}, a) = 1 - \prod_{n=1}^N [1 - P^{\text{obs}}(\mathbf{x}, A_p(M_n, D_n) > a)], \quad (4)$$

where  $P^{\text{obs}}(\mathbf{x}, A_p(M_n, D_n) > a)$  is the likelihood that the  $n$ th quake will generate accelerations greater than  $a$  at  $\mathbf{x}$ . Figure 5 remaps  $P_{150}^{\text{obs}}(\mathbf{x}, 0.1 \text{ g})$  and  $P_{150}^{\text{obs}}(\mathbf{x}, 0.2 \text{ g})$  including the 0.22 spread parameter. The new probability function is similar to that in Figure 2, but is smoother since it now can take all values between 0 and 1.

Ten areal averages  $P_{150}^{\text{obs}}(A_j, a)$  recomputed for the areas between adjacent predicted contours of Figure 3 are plotted versus the new  $P_{150}^{\text{pred}}(A_j, a)$  in Figure 6. Inclusion of the spread in the attenuation law increased the overall level of observed

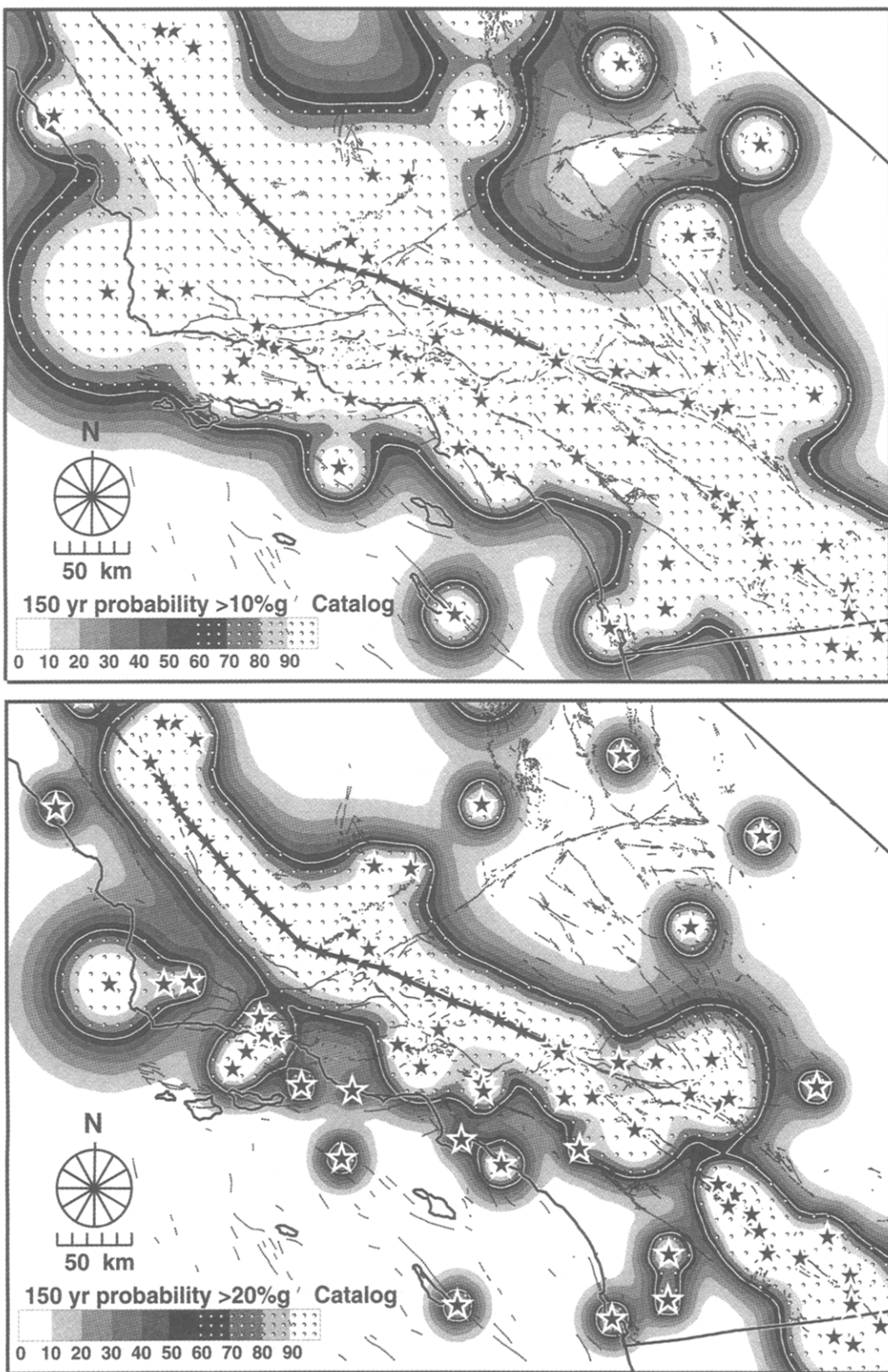


Figure 5. Observed 150-yr exceedence probabilities  $P_{150}^{\text{obs}}(\mathbf{x}, a)$  for accelerations of  $0.1 \text{ g}$  (top) and  $0.2 \text{ g}$  (bottom) based on the earthquake catalog and the Joyner and Boore (1981) attenuation curves including a random spread in  $\log [A_p(M, D)] = 0.22$ . Compare with Figure 2.

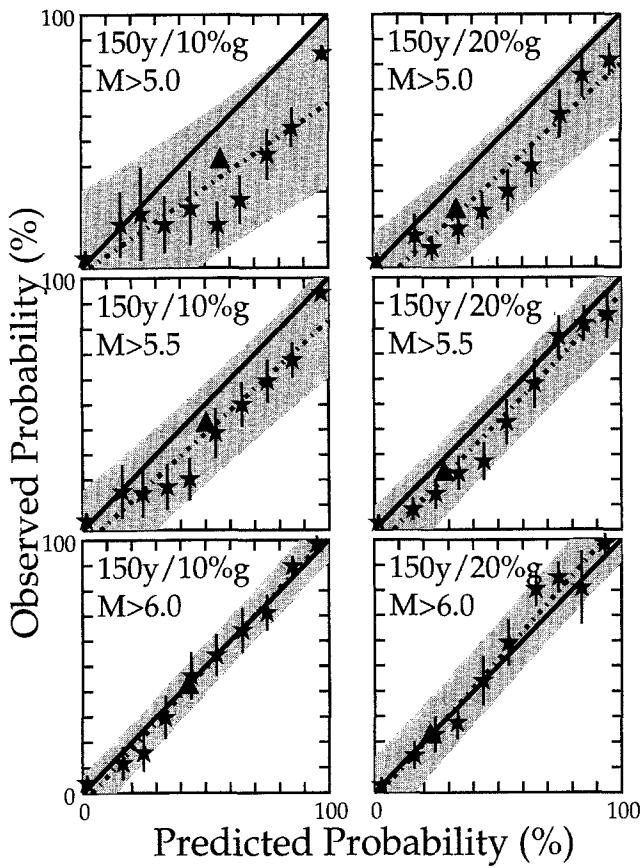


Figure 6. Observed versus predicted 150-yr area-averaged probabilities (Fig. 3 versus Fig. 5). Left and right columns are for accelerations of  $0.1\text{ g}$  and  $0.2\text{ g}$ . From top to bottom the rows test predictions with low-magnitude cutoffs of  $M \geq 5$ ,  $5.5$ , and  $6$ . Hazards predicted with a cutoff of  $M \geq 6$  fall well within the 95% confidence limits (shaded area) of the observations.

hazard. Strong support for the legitimacy of the predicted hazard map scaled to a 150-yr interval is offered by the nearly perfect agreement with the observed hazard for models with an  $M \geq 6$  cutoff. For  $M \geq 5.5$  and  $M \geq 5.0$  cutoffs, the model probabilities overpredict the Ellsworth catalog by about 20 and 30%, respectively.

### 30-Yr Probability–Probability Tests

To test the 30-year predictions directly, 30-year observed acceleration maps are needed. One way to obtain a  $P_{30}^{\text{obs}}(\mathbf{x}, a)$  is to scale  $P_{150}^{\text{obs}}(\mathbf{x}, a)$  using equation (3),

$$P_{30}^{\text{obs}}(\mathbf{x}, a) = 1 - [1 - P_{150}^{\text{obs}}(\mathbf{x}, a)]^{30/150}. \quad (5)$$

A second method would be to decimate the 150-earthquake catalog into 30-yr pieces, compute five estimates of  $P_{30}^{\text{obs}}(\mathbf{x}, a)$ , and then average. The probabilities obtained through equation (5), because of the nonlinear terms in the scaling,

will always be greater than or equal to the mean of the probabilities from the decimated catalog. Still, I expect scaling through equation (5) to give the smoothest overall picture, while decimation should give a better view of the uncertainty expected in any 30-yr sample of seismicity.

Figure 7 plots the observed exceedence probabilities scaled to 30 years by equation (5). Figure 8 plots the observed exceedence probabilities with  $a = 0.1\text{ g}$  for the five, 30-yr spans (1850 to 1880, 1880 to 1910, 1910 to 1940, 1940 to 1970, 1970 to the present) of the decimated catalog. Figures 9 and 10 plot area-averaged probabilities  $P_{30}^{\text{obs}}(A_j, a)$  versus  $P_{30}^{\text{pred}}(A_j, a)$  for the areas between adjacent predicted contours of Figure 1 for the scaled and decimated catalogs, respectively. Apart from several of the highest probability contours being absent, the 30-yr tests behave in the same fashion as the 150-yr tests. Specifically, observed hazard is found to correlate highly with predicted hazard and the predictions tend to be biased high when  $M < 5.5$  events are included. As in the 150-yr test, observed and predicted hazard values coincide at the 95% confidence level for magnitude cutoffs between 5.5 and 6, close to level where the catalog is complete.

To the extent that observational data are available, I conclude that the predicted hazard maps are fully consistent with the pattern, intensity, and frequency of historical earthquake shaking. Please note that in the construction of the multi-disciplinary maps, catalog seismicity was employed only to the extent of extracting a mean moment rate for all of southern California. The geography or sequencing of the quakes did not constrain the predicted probabilities, so this is a fair conclusion based on (relatively) independent information.

### A Pass/Fail Criterion

The widths of the 95% confidence limits in Figure 10 are nearly constant at approximately  $\pm 20\%$ . I interpret this spread as the intrinsic variability of peak accelerations associated with 30-yr samples of seismicity. Allowing for this variability, I propose a pass/fail criterion for acceleration hazard maps:

**Prediction:** of all points  $\mathbf{x}$  assigned a  $P\%$  probability of suffering accelerations exceeding  $a$  in the next 30 yr,  $P \pm 20\%$  of them will actually do so. **Test:** if more than 5% of such area ratios fall outside of these bounds, then the prediction can be considered a failure.

Of course, the acceleration data should be taken from, or corrected to, rock sites, and include quakes with magnitudes greater than the cutoff of the hazard map being tested. Tighter uncertainty bounds could be selected for the prediction, say  $\pm 10\%$ , with a corresponding increase (from 5%) in permitted violations. Likewise, time intervals shorter than 30 yr could be considered, but larger intrinsic variabilities in seismicity should be associated with the prediction. It also might be desirable to incorporate into the test bounds not

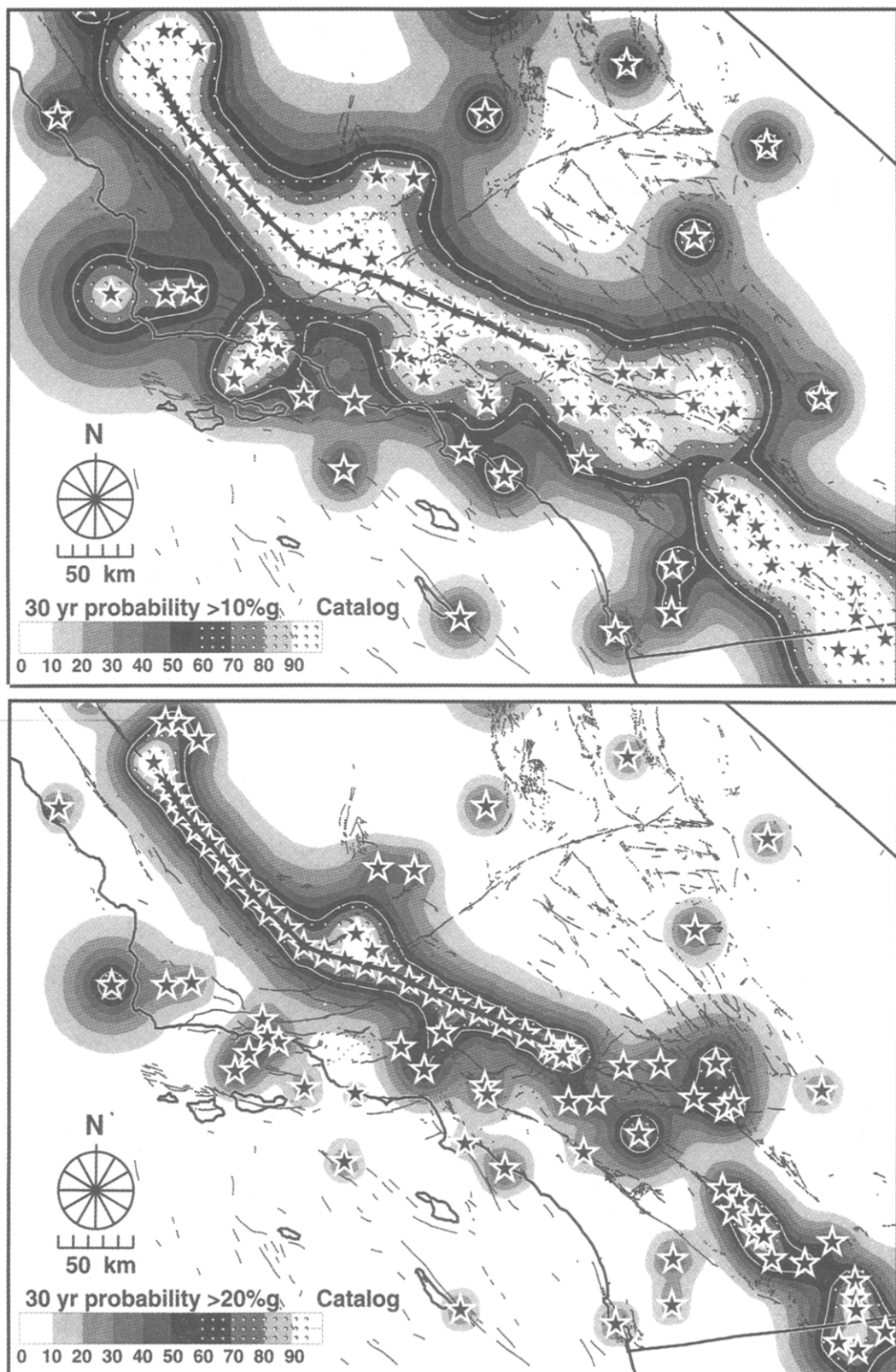


Figure 7. Observed 30-yr exceedance probability maps for accelerations of 0.1 g (top) and 0.2 g (bottom) based on the earthquake catalog and the Joyner and Boore (1981) attenuation curves, including a random spread in  $\log [A_p(M, D)] = 0.22$ . These probabilities were scaled from Figure 5 using equation (5). Compare with Figures 1a and 1b.

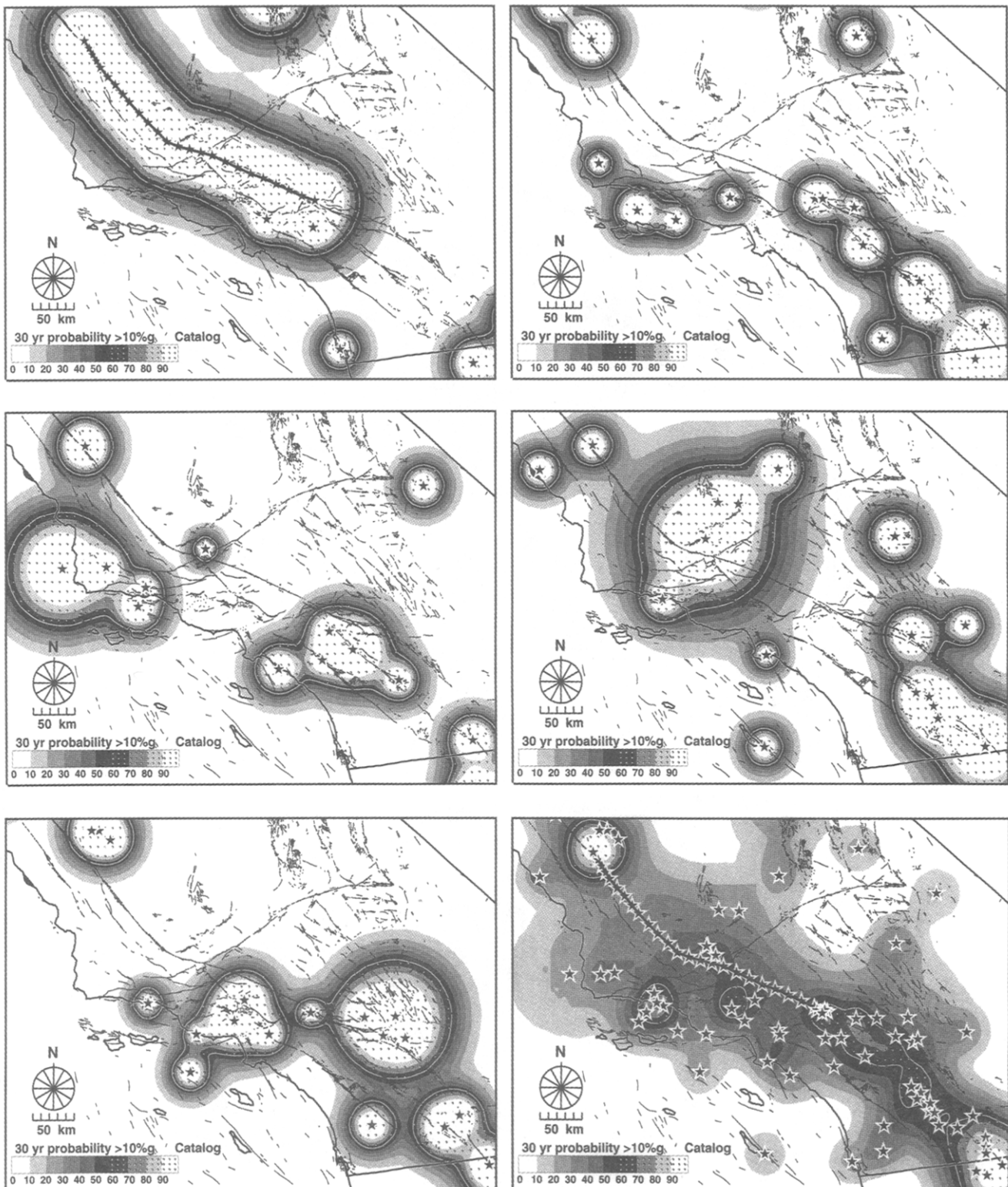


Figure 8. Observed 30-yr exceedence probability maps for accelerations of  $0.1\text{ g}$  based on the decimated earthquake catalog and the Joyner and Boore (1981) attenuation curves including a random spread in  $\log [A_p(M, D)] = 0.22$ . Left to right, top to bottom, the time spans include 1850 to 1880, 1880 to 1910, 1910 to 1940, 1940 to 1970, 1970 to 2000. The bottom right plot is the mean probability.

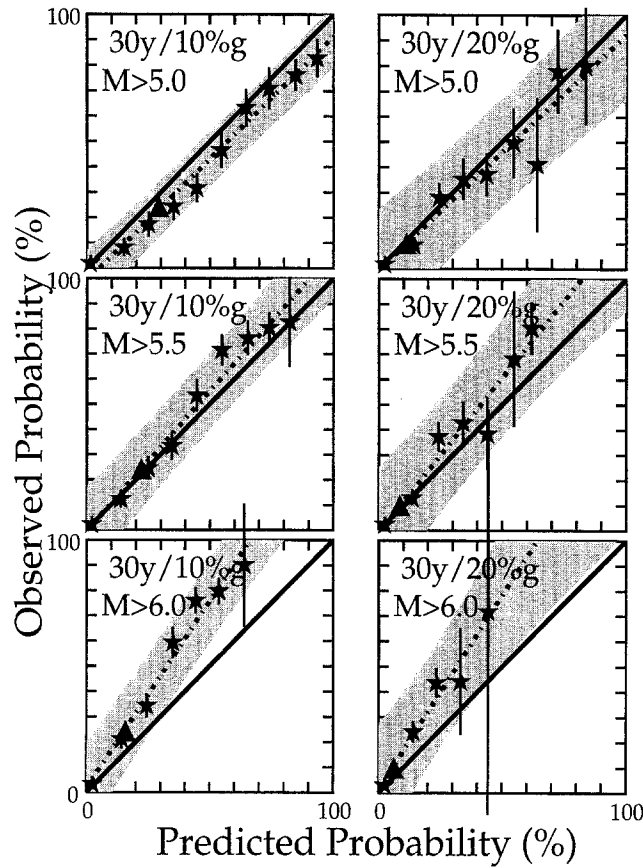


Figure 9. Observed versus predicted 30-yr area averaged probabilities (Fig. 1 versus Fig. 7). The observations come from scaling the 150-yr earthquake catalog to 30 yr by equation (5). Left and right columns are for accelerations of 0.1 g and 0.2 g. From top to bottom, the rows test predictions with low-magnitude cutoffs of  $M \geq 5$ , 5.5, and 6.

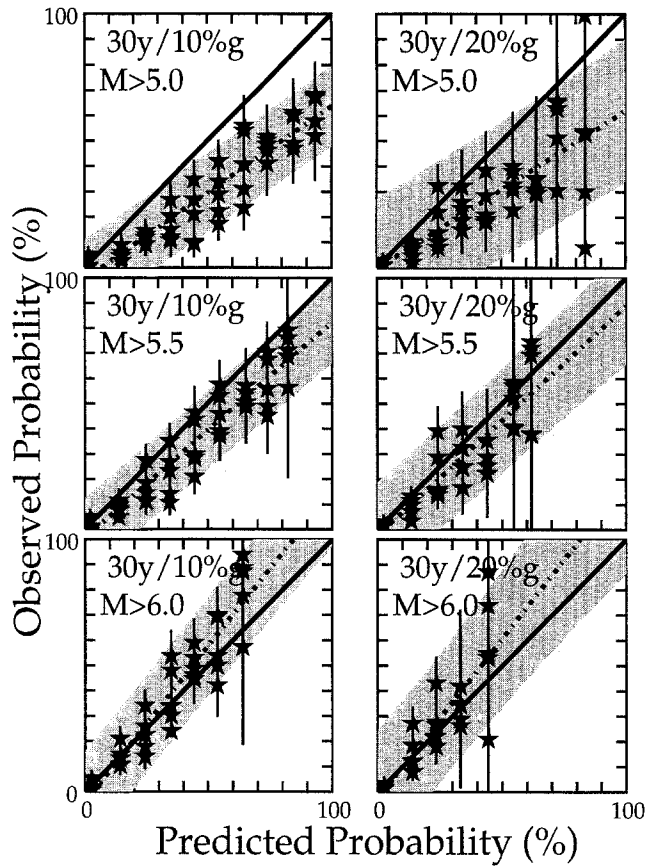


Figure 10. Observed versus predicted 30-yr area-averaged probabilities (Fig. 1 versus Fig. 8). The observations come from five consecutive 30-yr samples of the earthquake catalog. Left and right columns are for accelerations of 0.1 g and 0.2 g. From top to bottom, the rows test predictions with low-magnitude cutoffs of  $M \geq 5$ , 5.5, and 6.

only the intrinsic variability of seismicity, but the intrinsic uncertainty in the hazard model itself, if this could be quantified.

Although it is difficult to speculate on how wide of a community of acceleration hazard maps will simultaneously satisfy the criterion above, it does offer a fairly objective and time-durable test. I suggest that similar area-based tests be developed for other regions and other measures of hazard such as peak velocity, and that they be applied periodically as data availability warrants.

### Conclusions

This article responds to the challenge of testing long-term earthquake hazard predictions. The response exploits the areal extent of hazard maps to overcome the equivocality of traditional isolated earthquake predictions. The tests stem from the hypothesis that the observed fractional area of hazard exceedence should follow in proportion to the region's predicted likelihood of exceedence.

The absence of a long historical record of acceleration data on which to base the test was circumvented by generating observed exceedence maps from the 150-yr earthquake catalog and standard attenuation laws. Fabricating "observed" acceleration data may seem suspicious, but the input to the process, the earthquake catalog, is uncontroversial. If standard attenuation laws are realistic, then the constructed acceleration maps should be a reasonable representation of what would have been measured had instrumentation existed.

Overall, the long-term hazard maps from Ward (1994) fit remarkably well against both 150-yr and 30-yr estimates of observed accelerations. On an area-averaged basis, I find that observed geographical patterns of shaking are highly correlated with predicted patterns. Within 95% confidence bounds, the observed levels of hazard coincide with the predicted hazard for models with low-magnitude cutoffs equal to that of the catalog ( $M \approx 5.5$  to 6). By decimating the 150-yr catalog, I estimate a  $\pm 20\%$  intrinsic variability in acceleration probabilities for any 30-yr sample of seismicity. Al-

lowing for this variability, a time-durable pass/fail criterion for acceleration hazard maps can be constructed. Area-based tests should be applied to all earthquake hazard models, and periodically administered as field data accumulate.

In the end, no test can ever prove or disprove a statistical prediction; however, the ability of the existing acceleration hazard maps to satisfy a wide range of independent information encompassing GPS geodesy, fault geology, and observed seismicity, has to weigh in their favor.

### Acknowledgments

I thank Yan Kagan and Bob Youngs for their comments. This work was partially supported by the Southern California Earthquake Center project 569938 and NSF Grant Number EAR-9404962. Contribution 276, Institute of Tectonics, University of California, Santa Cruz, 95064.

### References

- Bakun, W. H. and A. G. Lindh (1985). The Parkfield, California earthquake prediction experiment, *Science* **229**, 619–624.
- Ellsworth, W. L. (1990). Earthquake history, in *The San Andreas Fault System, California, U.S. Geol. Surv. Profess. Pap. 1515*.
- Joyner, W. B. and D. M. Boore (1981). Peak horizontal accelerations and velocity from strong ground motion records including records from the 1979 Imperial Valley, California, earthquake, *Bull Seism. Soc. Am.* **71**, 2011–2038.
- Montgomery, D. C. and G. C. Runger (1994). *Applied Statistics and Probability for Engineers*, John Wiley and Sons Inc., New York.
- Ward, S. N. (1994). A multidisciplinary approach to seismic hazard in southern California, *Bull. Seism. Soc. Am.* **84**, 1293–1309.
- WGCEP (1988). Probabilities of large earthquakes occurring in California on the San Andreas fault, *U.S. Geol. Surv. Open-File Rept. 88-398*.
- WGCEP (1990). Probabilities of large earthquakes in the San Francisco Bay Region, California, *U.S. Geol. Surv. Circ. 1053*.
- Yerkes, R. F. (1985). Earthquake and surface-faulting sources, geologic and seismologic setting, *U.S. Geol. Surv. Profess. Pap. 1360*, 25 pp.

Institute of Tectonics  
University of California at Santa Cruz  
Santa Cruz, California 95064

Manuscript received 16 August 1994.